J|A|C|S ARTICLES

Published on Web 03/05/2009

Metal Clips That Induce Unstructured Pentapeptides To Be α-Helical In Water

Michelle T. Ma,[†] Huy N. Hoang,[‡] Conor C. G. Scully,[‡] Trevor G. Appleton,[†] and David P. Fairlie*[,‡]

School of Chemistry and Molecular Biosciences, and Institute for Molecular Bioscience, The University of Queensland, Brisbane Qld 4072, Australia

Received January 4, 2009; E-mail: d.fairlie@imb.uq.edu.au

Abstract: Short peptides corresponding to protein helices do not form thermodynamically stable helical structures in water, a solvent that strongly competes for hydrogen-bonding amides of the peptide backbone. Metalloproteins often feature metal ions coordinated to amino acids within hydrogen-bonded helical regions of protein structure, so there is a prospect of metals stabilizing or inducing helical structures in short peptides. However, this has only previously been observed in nonaqueous solvents or under strongly helix-favoring conditions in water. Here *cis*-$[Ru(NH_3)_4(solvent)_2]^{2+}$ and $[Pd(en)(solvent)_2]^{2+}$ are compared in water for their capacity as metal clips to induce α-helicity in completely unstructured peptides as short as five residues, Ac-HARAH-NH_2 and Ac-MARAM-NH_2. More α-helicity was observed for the latter pentapeptide and, when chelated to ruthenium, it showed the greatest α-helicity yet reported for a short metallopeptide in water (~80%). Helicity was clearly induced rather than stabilized, and the two methionines were 10^{13}-fold more effective than two histidines in stabilizing the lower oxidation state Ru(II) over Ru(III). The study identifies key factors that influence stability of an α-helical turn in water, suggests metal ions as tools for peptide folding, and raises an intriguing possibility of transiently coordinated metal ions playing important roles in native folding of polypeptides in water.

Introduction

Over 30% of amino acids in proteins exist in α-helical structures.[1] In metalloproteins, transition metal ions are often bound to α-helical protein segments.[2] When the helix is buried in the hydrophobic interior of a protein, metal−helix interactions can be important in stabilizing protein tertiary structure. When the helix is exposed on a protein surface, metal−helix interactions can shape either a catalytic site, a ligand binding cleft, or peptide domains that interact with macromolecules.[2,3] Despite extensive studies of metalloproteins and model metallopeptides, the capacity of metal ions to initiate or stabilize helical structures for short peptides in water remains obscure.[4,5] An intriguing question is whether a preformed peptide helix is stabilized by capture of a metal ion (Scheme 1, path a) or whether peptide helicity is induced following metal capture (Scheme 1, path b).

Scheme 1

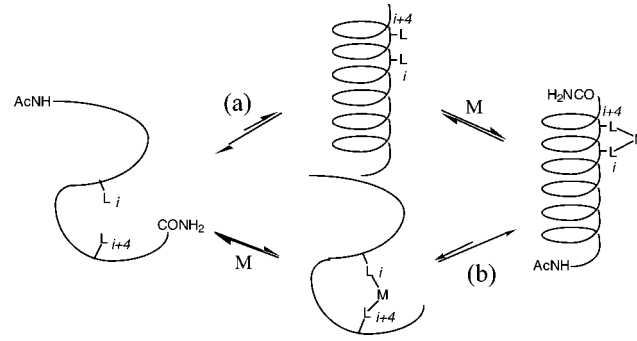

(a) Helix *stabilization* by metal (M) capture after helix formation versus (B) Helix *induction* after metal capture.

A significant problem in studying helices is that short synthetic peptides corresponding to helical segments (4−15 amino acids) of proteins are not thermodynamically stable helices in water, away from hydrophobic protein environments.[6]

[†] School of Chemistry and Molecular Biosciences.
[‡] Institute for Molecular Bioscience.

(1) (a) Barlow, D. J.; Thornton, J. M. *J. Mol* **1988**, *201*, 601. (b) Fairlie, D. P.; West, M. L.; Wong, A. K. *Curr. Med. Chem.* **1998**, *5*, 29–62. (c) Andrews, M. J.; Tabor, A. B. *Tetrahedron* **1999**, *55*, 11711–43. (d) Fletcher, S.; Hamilton, A. D. *Curr. Opin. Chem. Biol.* **2005**, *9*, 632–8.
(2) (a) *Metalloproteins in Bioactive Molecules*; Otsuka, S.; Yamanaka, T., Eds.; Elsevier: Tokyo, 1988; Vol. 8. (b) Xue, Y.; Okvist, M.; Hansson, O.; Young, S. *Protein Sci.* **1998**, *7*, 2099. (c) Holland, D. R.; Hausrath, A. C.; Juers, D.; Matthews, B. W. *Protein Sci.* **1995**, *4*, 1955.
(3) (a) Elrod-Erickson, M.; Rould, M. A.; Nekludova, L.; Pabo, C. O. *Structure* **1996**, *4*, 1171. (b) Cowan, J. A. *J. Inorg. Biochem.* **1993**, *49*, 171–175.
(4) (a) Ghadiri, M. R.; Fernholz, A. K. *J. Am. Chem. Soc.* **1990**, *112*, 9633–5. (b) Ghadiri, M. R.; Choi, C. *J. Am. Chem. Soc.* **1990**, *112*, 1630–2.
(5) (a) Ruan, F.; Chen, Y.; Hopkins, P. B. *J. Am. Chem. Soc.* **1990**, *112*, 9403–4. (b) Tofteng, A. P.; Hansen, T. H.; Brask, J.; Nielsen, J.; Thulstrup, P. W.; Jensen, K. J. *Org. Biomol. Chem.* **2007**, 2225–2233. (c) Kohn, W. D.; Kay, C. M.; Sykes, B. D.; Hodges, R. S. *J. Am. Chem. Soc.* **1998**, *120*, 1124–32. (d) Kohtani, M.; Kinnear, B. S.; Jarrold, M. F. *J. Am. Chem. Soc.* **2000**, *122*, 12377. (e) Kise, K. J., Jr.; Bowler, B. E. *Biochemistry* **2002**, *41*, 15826–37. (f) Nicoll, A. J.; Miller, D. J.; Fuetterer, K.; Ravelli, R.; Allemann, R. K. *J. Am. Chem. Soc.* **2006**, *128*, 9187–93.
(6) (a) Zimm, B. H.; Bragg, J. K. *J. Chem. Phys.* **1959**, *31*, 526–35. (b) Scholtz, J. M.; Baldwin, R. L. *Annu. Rev. Biophys. Biomol.* **1992**, *21*, 95–118.

This is because water strongly competes for hydrogen-bond donor NH and acceptor CO groups in a peptide backbone, which can otherwise hydrogen bond to one another to define an α-helix. Consequently, short peptides (<15 residues) are usually random, interconverting structures in water.[6] Two other problems are that most physiologically relevant metal ions are exchange labile, coordinating only transiently to short peptides *in vitro* or in different binding modes than in metalloproteins, and are usually paramagnetic, limiting potentially revealing solution structure studies by NMR spectroscopy.

Most of the few studies aimed at investigating whether metals induce α-helicity in short peptides have concerned peptides with greater than 15 amino acids with already appreciable helicity (e.g., Ala-rich) and/or conditions that are highly favorable to promoting helicity (low temperature, high ionic strength, nonaqueous solvents, unnatural constraints, etc).[4,5] Path a in Scheme 1 is most likely for these studies, in which metals have most often been assumed, rather than rigorously proven, to form macrocyclic chelates by coordinating two amino acid side chains separated by three intervening residues in a sequence (e.g., (*i*,*i*+4) positions as in His-xxx-His).[4,5] For example, *cis*-$[Ru(NH_3)_4(OH_2)_2]^{2+}$ reportedly[4a] reacts in situ with a 17 residue α-helical (45%) alanine-rich peptide (Ac-AEAAAKEAAA-KHAAAHA-NH_2) to form an exchange-inert metallopeptide with the air-oxidized form Ru(III) bound to two His residues, an α-helical backbone assigned on the basis of changes to circular dichroism spectra. No mention was made of linkage isomers as the result of the two histidines being able to coordinate via imidazole N1 and N3. In a related study,[4b] Cd^{2+} and Cu^{2+} showed similar stabilizing effects in peptides containing (*i*, *i* + 4) spaced His, His or Cys, His ligating residues. High-affinity, unnatural metal-binding amino acids such as those bearing aminodiacetic[5a] acid, pyridyl,[5b] or other side chains have also been suggested to stabilize helicity in the presence of metals, with varying degrees of stabilization depending on the metal, the spacing between ligating residues (*i*, *i* + 4 preferred), and the length of side chain. It was not definitively established how these various peptides bound to metal; only metal ions with octahedral coordination spheres were thought capable of promoting helicity, and square planar Pt(II) and Pd(II) reportedly destabilized helices.[4b,7]

We now focus on the more difficult task of inducing α-helicity in the much shorter pentapeptides that are not α-helical in water. This potentially permits an answer to the question of feasibility for path b in Scheme 1. We have shown that α-helix induction is feasible in a pentapeptide in an aprotic solvent (DMF) with no competing H-bond donors.[8] The pentapeptide Ac-HAAAH-NH_2 reacted with $[Pd(en)(ONO_2)_2]$ in DMF-d_7 to give three linkage isomers, coordinating via imidazole N1,N1 (**1**), N3,N1 (**2**), N1,N3 (**3**) in the ratio 2:1:0.7. 2D-NMR spectroscopy was used to determine a solution structure for the most abundant isomer (**1**), revealing a 22-membered metallacycle that was α-helical in DMF, though only ~20% α-helical in water.[8] A pentapeptide Ac-HELTH-NH_2 corresponding to the zinc-binding domain in the metalloprotein thermolysin also produced only ~20% α-helicity for $[Pd(en)(peptide)]^{2+}$ in water, despite replacing histidine (H) with histidine methylated at imidazole-N3 (H*) to direct all metal coordination via imidazole-N1 (corresponding to **1**) rather than the less preferred imidazole-N3.[9]

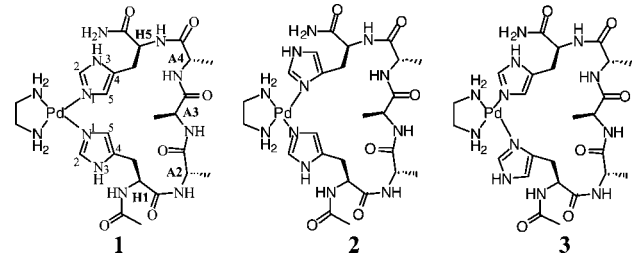

To better gauge the capacity of "metal clips" to *induce* α-helicity, we chose to make a direct comparison between exchange-inert diamagnetic metal ions, square planar *cis*-$[Pd(en)(solvent)_2]^{2+}$ and octahedral *cis*-$[Ru(NH_3)_4(solvent)_2]^{2+}$, for α helix induction in water-soluble pentapeptides with metal-ligating residues at positions *i* and *i* + 4. We also wished to determine the effect of replacing the histidine residues (H) by methionines (M), which could affect the flexibility of the macrochelate ring by altering ring size from 22-membered for the dominant N1,N1-bound isomer of a bis(histidine) metallopeptide to 20-membered for a bis(methionine) metallopeptide. We were unable to compare the previously studied Ac-HAAAH-NH_2 with Ac-MAAAM-NH_2, because the latter was not water soluble at millimolar concentrations required for NMR spectroscopy. We therefore replaced the central alanine with the water-solubilizing arginine (R), a residue with comparable helix-favoring properties to alanine. Similar xARAx pentapeptides have been found[10] to be good models for studying α-helicity in the absence of metals. The arginine side chain is not a metal-binding residue at physiological pH,[11] being protonated instead of metalated below pH 12. We thus chose to compare α-helix induction in the model pentapeptides Ac-HARAH-NH_2 (**4**) and Ac-MARAM-NH_2 (**5**). Using CD and NMR spectroscopy to analyze structure, this new study compares (a) the two metal ions, (b) the two coordinating residues, His and Met, in a pentapeptide sequence, and (c) 20−22 membered metallacycle products, for their capacities to stabilize α-helicity in water. The study identifies key factors in addition to peptide sequence that can influence the stability of a single α-helical peptide turn, one of the most important structural building blocks in proteins.

Results

Pentapeptides. An idealized α-helical turn is defined by 3.6 residues, a 13-membered NH···OC hydrogen-bond ring bringing together two residues separated by three intervening amino acids, and by a CHα···CHα nonbonding distance of <7 Å between the first and fifth residues. To accommodate these features, we focused on five-residue peptides with a putative metal-binding residue (His, Met) at each end, three residues apart at positions *i* and *i* + 4. Neither pentapeptide has any detectable α-helical structure on its own in water by CD and

(7) Parac, T. N.; Kostic, N. M. *Inorg. Chem.* **1998**, *37*, 2141.
(8) (a) Kelso, M. J.; Hoang, H. N.; Appleton, T. G.; Fairlie, D. P. *J. Am. Chem. Soc.* **2000**, *122*, 10488–9. (b) Hoang, H. N.; Bryant, G. K.; Kelso, M. J.; Beyer, R. L.; Appleton, T. G.; Fairlie, D. P. *Inorg. Chem.* **2008**, *47*, 9439–49.
(9) (a) Kelso, M. J.; Hoang, H. N.; Oliver, W.; Sokolenko, N.; March, D. R.; Appleton, T. G.; Fairlie, D. P. *Angew. Chem., Int. Ed.* **2003**, *42*, 421–4. (b) Kelso, M. J.; Beyer, R. L.; Hoang, H. N.; Lakdawala, A. S.; Snyder, J. P.; Oliver, W. V.; Robertson, T. A.; Appleton, T. G.; Fairlie, D. P. *J. Am. Chem. Soc.* **2004**, *126*, 4828–42. (c) Beyer, R. L.; Hoang, H. N.; Appleton, T. G.; Fairlie, D. P. *J. Am. Chem. Soc.* **2004**, *126*, 15096–105.
(10) Shepherd, N. E.; Hoang, H. N.; Abbenante, G.; Fairlie, D. P. *J. Am. Chem. Soc.* **2005**, *127*, 4828–42, and references therein.
(11) Fairlie, D. P.; Woon, T. C.; Wickramasinghe, W.; Skelton, B.; White, A.; Taube, H. *Inorg. Chem.* **1997**, *36*, 1020–1028.

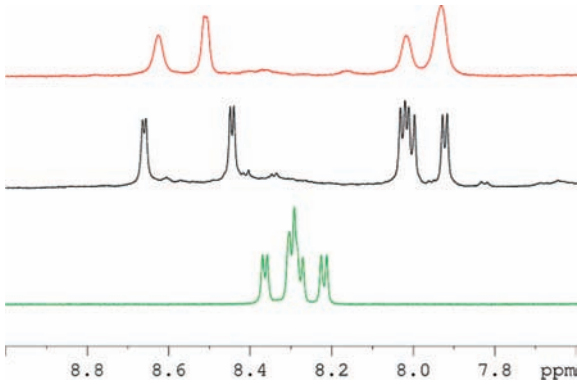

Figure 1. Amide NH region of the ^{1}H NMR spectra of **7** (red, top), **9** (black, middle), and **5** (green, bottom) in 9:1 H_2O:D_2O (pH 4).

NMR spectroscopy. We have previously shown[8] that HAAAH has some helical propensity in the presence of metal ions, alanine residues being well-known for supporting α-helical conformations.

Metal Coordination By Pentapeptides. While first row transition metals are most physiologically relevant to formation of α-helical metallopeptides *in vivo*, there are significant limitations to monitoring their complexes in water. Most are paramagnetic and form exchange-labile complexes in water with the metal only transiently coordinated, causing ^{1}H NMR spectra to show broad resonances of low resolution. We thus chose to study diamagnetic metal ions, *cis*-$[Pd(en)(solvent)_2]^{2+}$ and *cis*-$[Ru(NH_3)_4(solvent)_2]^{2+}$. Pentapeptides **4** and **5** were separately reacted with $[Pd(en)(OH_2)_2]^{2+}$ and *cis*-$[Ru(NH_3)_4(OH_2)_2]^{2+}$, generated in situ in water, to give metallopeptides **6**−**9**, which were characterized by proton NMR spectroscopy (Supporting Information).

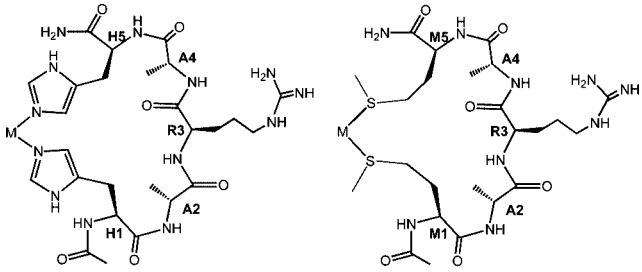

1D and 2D proton NMR spectra for *cis*-$[Ru(NH_3)_4(OH_2)_2]^{2+}$ and *cis*-$[Pd(en)(OH_2)_2]^{2+}$, mixed separately with Ac-MARAM-NH_2 (**5**) in water, each showed only one set of signals (Figure 1), indicating a single species formed, [Pd(en)(1,5-Ac-MARAM-NH_2)]$^{2+}$ (**7**) and *cis*-$[Ru(NH_3)_4$(1,5-Ac-MARAM-NH_2)]$^{2+}$ (**9**), respectively,[12] in which the peptide is bound to metal through two methionine-S atoms forming a 20-membered macrocycle.

While peptide **5** was unstructured in water with amide NH resonances clustered together (Figure 1, bottom), both metal complexes **7** and **9** showed amide NH resonances dispersed over 0.8 ppm, the greater dispersion being indicative of induced

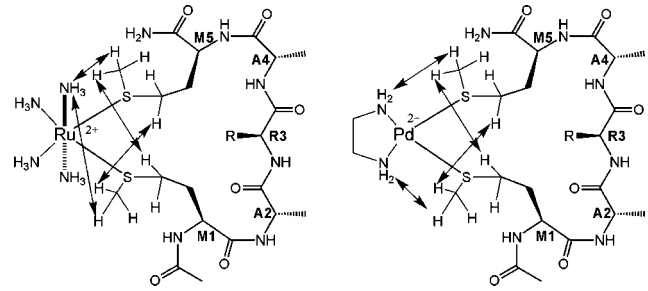

Figure 2. Compounds **9** and **7** showing some observed NOEs (two headed arrows) between Met side chains and *cis*-$[Ru(NH_3)_4]^{2+}$ and $[Pd(en)]^{2+}$, respectively, which establish the binding mode of the peptide.

structure (Figure 1). In principle, isomers of these compounds are possible, depending on the configurations about the sulfur atoms. Presumably, inversion at sulfur is fast enough for only one set of peaks to be observed, although incomplete averaging may be responsible for the broadness of some peaks in the spectra of the palladium compound. ROESY spectra of **7** and **9** each showed ROE correlations between methyl protons from the two methionine side chains and between the metal-bound amines to these same methyl protons, establishing metal coordination via sulfur atoms forming 20-membered metallacycles (Figure 2).

As with previously reported Ac-HAAAH-NH_2,[8] peptide **4** (Ac-HARAH-NH_2) can bind to a metal ion through either imidazole N1 or N3 of either histidine, thereby potentially forming four linkage isomers, [M{1,5-Ac-H(N1)ARAH(N1)-NH_2}]$^{2+}$, [M{1,5-Ac-H(N1)ARAH(N3)-NH_2}]$^{2+}$, [M{1,5-Ac-H(N3)ARAH(N1)-NH_2}]$^{2+}$, and [M{(1,5-Ac-H(N3)ARAH(N3)-NH_2}]$^{2+}$, resulting in 20−22-membered macrocycles. All four isomers were detected in the reaction of *cis*-$[Ru(NH_3)_4(OH_2)_2]^{2+}$ with **4**. The reaction of **4** with $[Pd(en)(OH_2)_2]^{2+}$ gave only three isomers, the major isomer being **6**. NMR peaks due to particular linkage isomers (Supporting Information) were assigned as described previously for the Ac-HAAAH-NH_2 isomers.[8]

Helix Stabilization by Metal Clips. CD spectra for **4** and **5** were characteristic[13] of unstructured peptides with a strong negative minimum at 190−200 nm (Figure 3, top), whereas α-helical polypeptides typically display a maximum at 190 nm and double minima at 208 and 222 nm (at lower λ for short peptides[10]). CD spectra for **6** and **8** suggest a mixture of random coil and helical conformers. As discussed above, the solutions containing **6** and **8** contained multiple linkage isomers with different structures, and the CD spectra are composites of these structures. However, **7** and **9** exhibit more helix-like CD spectra (Figure 3, top). The deeper minimum at 207 nm for **7** might suggest 3_{10}-helicity rather than α-helicity,[14] whereas **9** exhibits the strongest α-helix character. Relative helicities calculated (Experimental Section) from the mean residue ellipticity at 218 nm (Figure 3, top) were 14% (**6**), 76% (**7**), 17% (**8**), and 82% (**9**).

We also compare CD spectra in Figure 3 (bottom) for *cis*-$[Ru(NH_3)_4$(Ac-HARAH-NH_2)]$^{2+}$ and *cis*-$[Ru(NH_3)_4$(Ac-MARAM-NH_2)]$^{2+}$ (**9**) with those of the "intermediate" compounds *cis*-$[Ru(NH_3)_4$(Ac-MAAAH*-NH_2)]$^{2+}$ (**10**) and *cis*-$[Ru(NH_3)_4$-(H*AAAM)]$^{2+}$ (**11**),[12] in which H* indicates N3-methylhisti-

(12) To avoid confusion over the oxidation state of the metal and the pH being monitored, we adopt normal convention in showing peptides as neutral or uncharged ligands either alone or in metal complexes, even through the Arg/Lys side chains are protonated in water at pH <9, His side chain is protonated at pH >7, and Asp/Glu side chains are deprotonated at pH >5.

(13) Chin, D. H.; Woody, R. W.; Rohl, C. A.; Baldwin, R. L. *Proc. Natl. Acad. Sci. U.S.A.* **2002**, *99*, 15416–21.

(14) (a) Zhou, N. E.; Kay, C. M.; Hodges, R. S. *Biochemistry* **1992**, *31*, 5739–46. (b) Garcia-Echeverria, C. *J. Am. Chem. Soc.* **1994**, *116*, 6031–2.

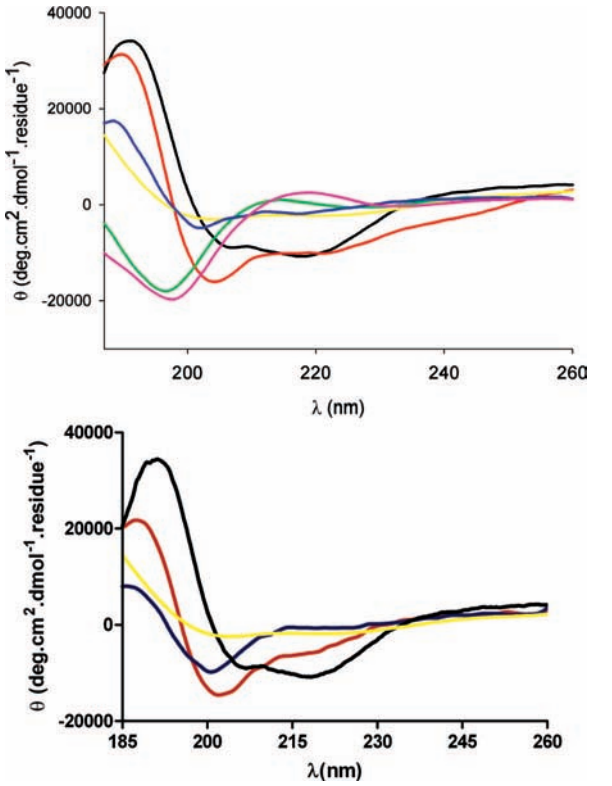

Figure 3. CD spectra of metallopeptides in sodium acetate buffer (10 mM) at pH 4. (Top) Comparison of compounds **4** (magenta), **5** (green), **6** (blue), **7** (red), **8** (yellow), and **9** (black). (Bottom) Comparison of compounds **8** (yellow), **9** (black), **10**(blue), and **11** (red).

dine, which was used to direct coordination of Ru(II) to just the N1-nitrogen of histidine. There was a nice gradation of α-helical content ranging from 17% (**8**), 16% (**10**), 47% (**11**), to 82% (**9**). This data suggests that histidines are less effective than methionines in promoting an α-helical conformation in the pentapeptide backbone.

The most α-helical metallopeptides **7** and **9** were subjected to further scrutiny of their structures by more detailed ^{1}H NMR spectroscopic studies. The Supporting Information shows that all CHα proton resonances for **7** and **9** were shifted upfield relative to those of free peptide **5** (Supporting Information, Figure S4), consistent with α-helicity:[15] the NH proton of M5 and one of the terminal NH_2 protons displayed temperature-independent chemical shifts $\Delta\delta/T \leq 4$ ppb/K (Supporting Information, Figure S3), as expected for hydrogen bonds in an α-helix,[16] and $^3J_{NHCH\alpha} < 6$ Hz for four residues in **9** (Supporting Information, Table S1), typical of α-helicity.[17] However, amide NH resonances for **7** were too broad to observe $^3J_{NHCH\alpha}$ coupling constants.

2D ROESY spectra were acquired for **7** and **9** generated *in situ*. For **9** there were sequential ROEs ($d_{NN}i,i+1$; $d_{\alpha N}i,i+1$) and numerous medium range ROEs indicative of α-helicity (Figures 4 and 5).[18] For **7**, two key sequential ROE signals ($d_{NN}i,i+1$ signals) were missing and only one medium range ROE was

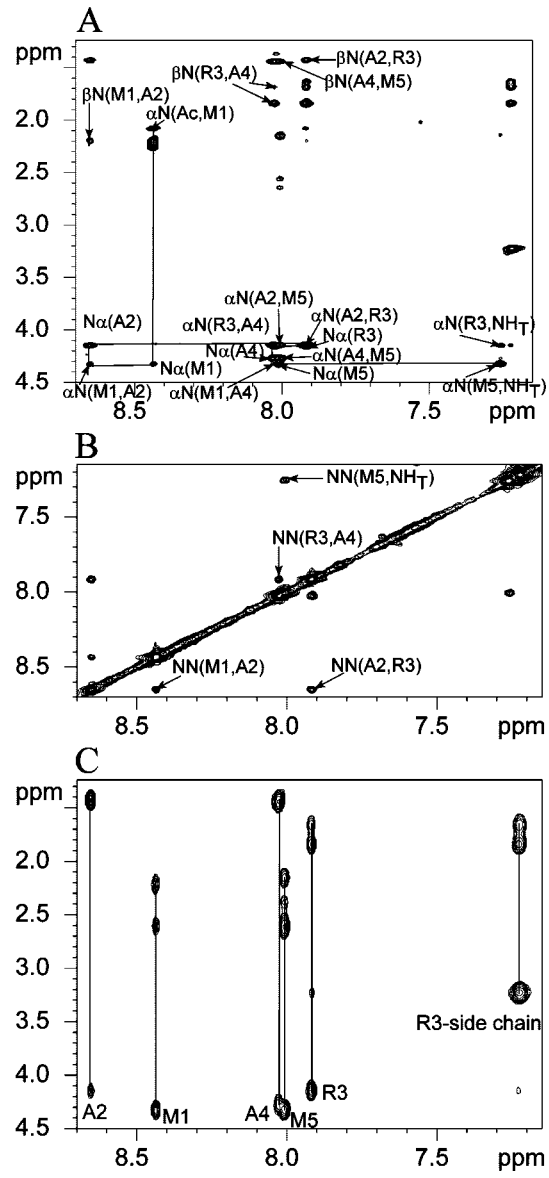

Figure 4. 2D NMR spectra for *cis*-$[Ru(NH_3)_4(Ac\text{-}MARAM\text{-}NH_2)]^{2+}$ (**9**)[12] in H_2O with 10% D_2O, pH 4. (A) ROESY spectrum, α to N region; (B) ROESY spectrum, N to N region; (C) TOCSY spectrum, N to N region.

observed (Figure 5). In water, the Ru(II) compound **9** has greater α-helicity than the Pd(II) analogue **7**. CD spectra for **7** also hinted at some 3_{10}-helical character based on the reduced molar ellipticity at 222 nm.

A solution structure was calculated for **9** in H_2O/D_2O (9:1), using a dynamic simulated annealing and energy minimization protocol in X-PLOR,[19] from 48 NOE distance restraints (22 intraresidue, 18 sequential, 8 medium-long-range) and four backbone ϕ-dihedral angle restraints. Coordinating M1 and M5 sulfur atoms were constrained to a distance of 3.4 Å, conforming to typical crystal structure data.[20] Two hydrogen-bond restraints were used (for NH protons with $\Delta\delta T \leq 4$ ppb/K) to calculate the 20 lowest energy structures of **9**, shown in Figure 6 as a tight α-helical turn (rmsd 0.366 Å, peptide backbone).

(15) Wishart, D. S.; Sykes, B. D.; Richards, F. M. *J. Mol. Biol.* **1991**, *222*, 311–33. Wishart, D. S.; Sykes, B. D.; Richards, F. M. *Biochemistry* **1992**, *31*, 1647–51.
(16) (a) Kessler, H. *Angew. Chem.* **1982**, *21*, 512–523. (b) Dyson, H. J.; Cross, K. J.; Houghten, R. A.; Wilson, I. A.; Wright, P. E.; Lerner, R. A. *Nature* **1985**, *318*, 480–3.
(17) Dyson, H. J.; Wright, P. E. *Annu. Rev. Biophys. Biophys. Chem.* **1991**, *20*, 519–38.
(18) Bradley, E. K.; Thomason, J. F.; Cohen, F. E.; Kosen, P. A.; Kuntz, I. D. *J. Mol. Biol.* **1990**, *215*, 607–22.
(19) Brunger, A. T. *X-PLOR Version 3.1*; Yale University: New Haven, CT, 1992.

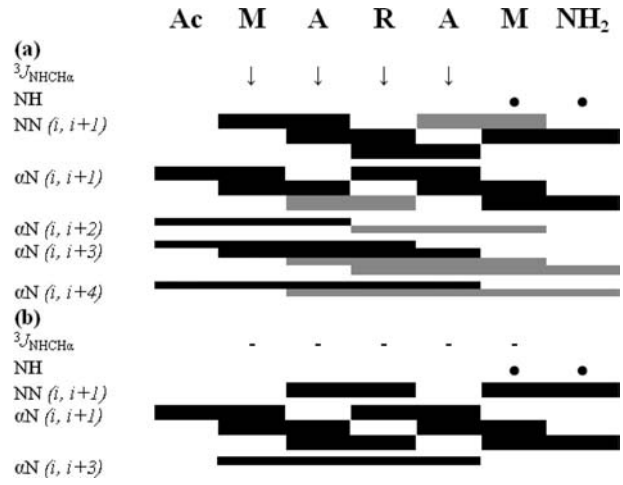

Figure 5. NMR summary for (a) **9** and (b) **7** of sequential and medium-range ROEs, the bar thickness being proportional to strong (upper distance constraint 2.7 Å), medium (3.5 Å), weak (5.0 Å), and very weak (6.0 Å) ROE intensities. Overlapping crosspeaks are gray bars; $^3J_{NHCH\alpha} \leq 6$ Hz (↓); amide NH chemical shifts ($\Delta\delta$) ≤ 4 ppb/K (●).

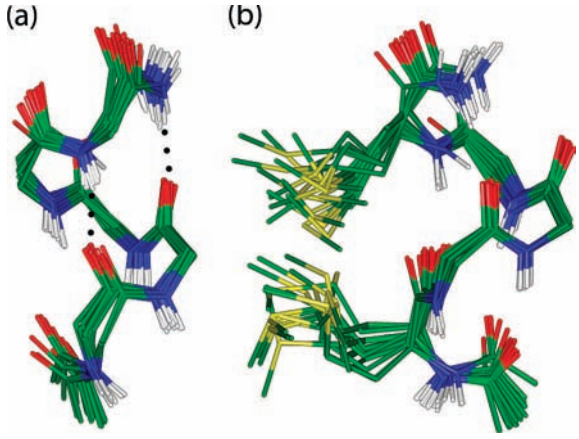

Figure 6. Backbone superimposition of 20 lowest energy refined structures of **9** with hydrogen bonds represented by dotted black lines (red, oxygen; blue, nitrogen); peptide side chains and metal clip are omitted for clarity. (b) Peptide backbone of **9** with methionine side chains shown.

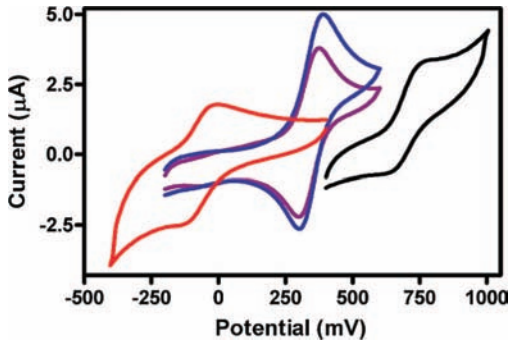

Figure 7. Cyclic voltammograms in H_2O (50 mV/s, pH 7.4, 100 mM $NaClO_4$) vs Ag/Ag^+ for 2 mM *cis*-$[Ru(NH_3)_4(peptide)]^{2+}$ generated in situ, where peptide = Ac-HARAH-NH_2 (**8**, red), Ac-MARAM-NH_2 (**9**, black), Ac-H*AAAM-NH_2 (**10**, blue), and Ac-MAAAH*-NH_2 (**11**, purple).[12]

Reversible cyclovoltammograms (Figure 7) support both (i) the observed ready oxidation of **8** in air to Ru(III) ($E^{1/2} = -70 \pm 10$ mV, pH 7.6, Ag/AgCl) and (ii) the contrasting air-stable Ru(II) oxidation state in **9** ($E^{1/2} = 700 \pm 10$ mV, pH 7.2, Ag/AgCl). This substantial difference in reduction potentials for

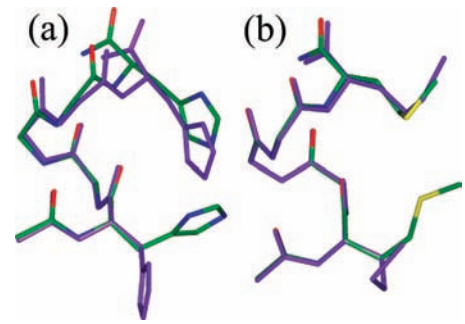

Figure 8. Comparison of unconstrained (purple) vs constrained (green) energy-minimized helical backbone conformations for (a) peptide **4** and (b) peptide **5**. Distance constraints used were 2.8 ± 0.1Å between two nitrogen (N1) atoms in **4** and 3.4 ± 0.1 Å between two sulfur atoms in **5**.

Ru(III) ($\Delta E = 770$ mV) translates to a free energy (ΔG) difference[21] between complexes **8** and **9** of ∼74.3 kJ/mol, revealing that Ru(II) is stabilized over Ru(III) by the two methionines versus the two histidines by a factor of 10^{13}. This stabilization of the Ru(II) oxidation state by methionines is attributed to Ru(II)→S π^{*22a} or σ^{*22b} back-bond stabilization afforded by the thioether of methionine. We note that reported equilibrium constants[22c] for water substitution by the thioether Me_2S in water at 25 °C for $[Ru(NH_3)_5(OH_2)]^{2+}$ versus $[Ru(NH_3)_5(OH_2)]^{3+}$ are $\geq 10^5$ versus 1.6×10^{-2}, which is a ratio of at least 6×10^6 in favor of Ru(II) over Ru(III) for one thioether sulfur ligand only compared with two thioether sulfur atoms in **9**. We also compared cyclovoltammagrams (Figure 7) for the intermediate coordination modes *cis*-$[Ru(NH_3)_4$(Ac-MAAAH*-$NH_2)]^{2+}$ (**10**) and *cis*-$[Ru(NH_3)_4$(Ac-H*AAAM-$NH_2)]^{2+}$ (**11**). As expected, the formal reduction potential for each compound was midway between that for compounds **8** and **9**.

We briefly investigated the origin of the enhanced helicity induced by the metal clips in Ac-MARAM-NH_2 (**5**) versus Ac-HARAH-NH_2 (**4**) by examining computer model simulations (Figure 8). Idealized α-helical peptides with these sequences were generated and energy minimized in SYBYL using Tripos force fields (Figure 8, purple). Distances between the two His-N1 atoms in **4** and two Met sulfur atoms in **5** were 6.79 and 7.02 Å, respectively. These distances were then restrained to 2.8 ± 0.1 Å and 3.4 ± 0.1 Å, on the basis of crystal structures for like compounds,[20] to simulate the binding of Ru(II) as in complexes **8** and **9**, respectively. The constrained peptides were also energy minimized (Sybyl, Tripos force field with Powell method of 1000 cycles and 0.05 kcal/mol gradient), and the total energies of each peptide were collected and compared for unconstrained vs constrained. There was a small reduction in energy (0.61 kcal/mol) for **4** when the two histidine side chains

(20) (a) Sheldrick, W. S.; Exner, R. *J. Organomet. Chem.* **1990**, *386*, 375–87. (b) Henderson, W.; Nicholson, B. K.; Oliver, A. G.; Clifton, E. F.; Rickard C. E. F., *J. Organomet. Chem.* **2001**, *625*, 40–46. (c) Henderson, W.; Kilpin, T. D.; Nicholson, B. K. *Struct. Chem.* **2008**, *19*, 199–202.

(21) $\Delta G = -nFE$, where $n = 1$ and $F = 9.648 \times 10^4$ C mol^{-1} (Faraday constant). For **8**, $E = 70$ mV; therefore, $\Delta G = -1.6$ kcal/mol. For **9**, $E = -700$ mV; therefore, $\Delta G = 16$ kcal/mol. The free energy difference between **8** and **9** then equals $16-(-1.6) = 17.7$ kcal/mol or 74 kJ/mol.

(22) (a) Taube, H. *Pure Appl. Chem.* **1979**, *51*, 901–12. (b) Jacobsen, H.; Kraatz, H. B.; Ziegler, T.; Boorman, P. M. *J. Am. Chem. Soc.* **1992**, *114*, 7851–60. (c) Kuehn, C. G.; Taube, H. *J. Am. Chem. Soc.* **1976**, *98*, 689–702.

were constrained, versus 1.17 kcal/mol for **5** when the two methionines were constrained. Superimposition of unconstrained and constrained peptides (Figure 8) gave rmsd 0.062 and 0.025 Å for histidine and methionine peptides, respectively. The constraint thus induces a much bigger deviation in the backbone for residue H5 in **4** than for residue M5 in **5** (Figure 8). The larger relative reduction in energy and smaller rmsd for **5** than **4**, upon restraining the side chains to mimic the effect of binding to ruthenium, is consistent with the helical peptide backbone in **9** being thermodynamically more stable than in **8**. It is clear that the two imidazole constraints impose greater restraint on the peptide backbone helix than the two more flexible methionine side chains.

Discussion

Metal ions have some capacity to stabilize peptides in a helical conformation through binding to side chains of two histidines[4,5,8,9] or one cysteine and one histidine[4b] three residues apart. This effect is however limited in water, which competes very strongly for hydrogen-bonding amides, and peptides are often 3_{10}-helical rather than α-helical. Here we show that methionines are much more effective than histidines and that *cis*-$[Ru(NH_3)_4(solvent)_2]^{2+}$ is more effective than *cis*-$[Pd(en)(solvent)_2]^{2+}$ in inducing α-helicity in five-residue peptides. The finding of >80% α-helicity for compound **9** is by far the most stable single turn of an α-helix reported to date for a small metallopeptide in water.[4,5,8,9]

As discussed earlier, most previous studies of helicity in peptides have involved sequences that were already appreciably α-helical before interaction with metal ions.[4,5] Thus, any increase in α-helicity detected by circular dichroism changes could be attributed to stabilization of helical structure rather than necessarily helix induction (Scheme 1, path a rather than b). In the present work, the pentapeptides show no discernible evidence of structure in water prior to addition of metals, yet in the most spectacular case up to 80% α-helicity has been measured by CD spectroscopy upon metal binding. Thus, it is most likely that α- helicity has been induced rather than merely stabilized (Scheme 1, path b rather than a) by the metal clips used herein. Furthermore, the NMR studies herein also unambiguously identify α-helicity rather than 3_{10}-helicity and thus are much more reliable than previous studies that have reported "α-helix induction" based only upon increased molar elipticity at 222 nm in CD spectra, which is associated with both helix structures.

Histidine is one of the most common amino acids found bound to metal ions in biological systems,[1] yet the presence of two imidazole nitrogens raises the possibility of linkage isomerism[8] in which either nitrogen can coordinate to a metal ion. We have found that both octahedral *cis*-$[Ru(NH_3)_4(OH_2)_2]^{2+}$ and square planar *cis*-$[Pd(en)(OH_2)_2]^{2+}$ can indeed coordinate to either of the imidazole nitrogens, resulting in four possible linkage isomers, only one of which[8] favors α-helical induction in pentapeptides. This suggests that helix induction in histidine-containing peptides is compromised by indiscriminate imidazole binding to metal ions. On the other hand, methionine-containing peptides have no such linkage isomerism complication. A further advantage of methionine over histidine in peptides is its capacity to stabilize lower oxidation states of metal ions, as exhibited here where the electrochemical parameters suggest a difference of 10^{13} for MARAM over HARAH in their respective stabilization of Ru(II) over Ru(III). This stabilizing effect might be particularly useful in studies of interactions between short peptides and biologically important transition metals, which tend to be maintained in lower oxidation states under the reducing conditions of biological milieu.

The success of this metal-clip approach to stabilizing an α-helical turn is due to the 20−22 membered metallopeptide rings, which favor formation of the two intramolecular hydrogen bonds that help define the α-turn. This ring size is not uncommon in metalloproteins,[23] although short peptides usually favor five- and six-membered rings in their interactions with metals.[24] Given that peptides tend to need 25 or more amino acids[6,13] before they show a high degree of α-helicity in water (more than six helical turns with three intramolecular hydrogen bonds per helical turn), the stabilization energy provided by the metal clips must be substantial. The molecular modeling study herein established that the cyclic metallopeptide formed by the metal clip is less strained for a *cis* Met-Ru-Met (20-membered ring) than a corresponding His-Ru-His (20−22 membered rings) chelate, reflecting the constraining impact of the imidazole rings.

Although we know of no crystallographically characterized metalloprotein in which two methionines of an α-helix bind to a metal, there are >100 examples of the MxxxM sequence within α-helical regions of proteins in the Swiss-Protein database, and it seems plausible that transient, reversible, methionine coordination to metal ions *in vivo* could help template helix folding in proteins. Longer peptides will need to be investigated *in vitro* to learn whether such metal clips can be used as folding tools to induce α-helicity and then be removed following their use as prospective folding chaperones.

Experimental Section

$[Pd(en)(ONO_2)_2]$. $[Pd(^{15}en)Cl_2]$ was prepared according to a literature method.[25] The dichloro complex was dissolved in water and stirred with 2.2 equiv of $AgNO_3$ in the dark at 60 °C for 2 h and then at room temperature for a further 24 h. The AgCl precipitate was removed by gravity filtration and the filtrate concentrated by gentle heating on a hot plate to yield a residue of $[Pd(en)(ONO_2)_2]$ as a yellow solid (73%). Anal. Calcd for $C_2H_8N_4O_6Pd$: C, 8.27; H, 2.78; N, 19.28. Found: C, 8.25; H, 2.73; N, 18.72.

$[Pd(en)(peptide)]^{2+}$ and *cis*-$[Ru(NH_3)_4(peptide)]^{2+}$. Compounds **6** and **7** were prepared by addition of $[Pd(en)(ONO_2)_2]$[9b] to **4** and **5**, respectively, in water. Compounds **8** and **9** were prepared by reduction of *cis*-$[Ru(NH_3)_4Cl_2]Cl$[26] to *cis*-$[Ru(NH_3)_4(H_2O)_2]^{2+}$ using zinc amalgam, in the presence of **4** and **5** respectively, in water. In the preparation of **8**, the solution was adjusted to pH 6−7 using

(23) (a) Magnus, K. A.; Hazes, B.; Ton-That, H.; Bonaventura, C.; Bonaventura, J.; Hol, W. G. *Proteins* **1994**, *19*, 302. (b) Holland, D. R.; Hausrath, A. C.; Juers, D.; Matthews, B. W. *Protein Sci.* **1995**, *4*, 1955. (c) Elrod-Erickson, M.; Rould, M. A.; Nekludova, L.; Pabo, C. O. *Structure* **1996**, *4*, 1171. (d) Morgunova, E.; Tuuttila, A.; Bergmann, U.; Isupov, M.; Lindqvist, Y.; Schneider, G.; Tryggvason, K. *Science* **1999**, *284*, 1667.

(24) (a) Agarwal, R. P.; Perrin, D. D. *J. Chem. Soc., Dalton Trans.* **1976**, 89. (b) Livera, C. E.; Pettit, L. D.; Battaaille, M.; Perly, B.; Kozlowski, H.; Radomska, B. *J. Chem. Soc., Dalton Trans.* **1987**, 661. (c) Ueda, J.; Ikota, N.; Hanaki, A.; Koga, K. *Inorg. Chim. Acta* **1987**, *135*, 43. (d) Sovago, I. In *Biocoordination Chemistry, Coordination Equilibria in Biologically Active Systems*; Ellis Horwood: London, 1990. (e) Tsiveriotis, P.; Hadjiliadis, N.; Savropoulos, G. *Inorg. Chim. Acta* **1997**, *261*, 83. (f) Milinkovic, S. U.; Parac, T. N.; Djuran, M. I.; Kostic, N. M. *J. Chem. Soc., Dalton Trans.* **1997**, 2771. (g) Kozlowski, H.; Bal, W.; Dyba, M.; Kowalik-Jankowska, T. *Coord. Chem. Rev.* **1999**, *184*, 319. (h) Hahn, M.; Wolters, D.; Sheldrick, W. S.; Hulsbergen, F. B.; Reedijk, J. *J. Biol. Inorg. Chem.* **1999**, *4*, 412. (i) Tsiveriotis, P.; Hadjiliadis, N. *J. Chem. Soc., Dalton Trans.* **1999**, 459.

(25) McCormack, J. B.; Jayes, E. N.; Kaplan, R. I. *Inorg. Synth.* **1972**, *13*, 216.

0.1 M NaOH (several 5 μL aliquots). The ruthenium−peptide solutions were allowed to react overnight.

Peptide Synthesis. Fmoc-N3-Me-His-OH was obtained from Bachem AG (Switzerland). Rink amide MBHA resin and other Fmoc-L-amino acids (Fmoc-Ala-OH, Fmoc-Met(OtBu)-OH, Fmoc-His-OH, Fmoc-Arg(Bzl)-OH were purchased from Novabiochem (Melbourne, Australia). 2-(1*H*-benzotriazol-1-yl)-1,1,3,3-tetramethyluronium hexafluorophosphate (HBTU) was obtained from Richelieu Biotechnologies (Quebec, Canada). All other reagents were of peptide synthesis grade and obtained from Auspep (Melbourne, Australia). Semipreparative rp-HPLC purification of the linear peptides was performed using a Waters Delta 600 chromatography system fitted with a Waters 486 tunable absorbance detector with detection at 254 and 214 nm. Purification was performed by eluting with solvents A (0.1% TFA in water) and B (9:1 CH_3CN:H_2O, 0.1% TFA) on a Vydac C18 250 × 22 mm (300 Å) steel jacketed column run at 20 mL/min. Analytical rp-HPLC analyses were performed using a Waters 600 chromatography system fitted with a Waters 996 photodiode array detector and processed using Waters Millenium software. Analytical analyses were performed using gradient elutions with solvents A and B on a Vydac C18 4.6 × 250 mm (300 Å) column. Peptide and protein columns were run at 1.0 mL/min. The peptides were synthesized manually by standard solid phase methods using HBTU/DIPEA activation for Fmoc chemistry on Rink Amide MBHA resin (substitution 0.72 mmol g^{-1}, 0.25 mmol scale syntheses, 350 mg of resin). Four equivalents of Fmoc-protected amino acids, 4 equiv of HBTU, and 2 equiv of DIPEA were employed in each coupling (except for coupling of Fmoc-N3-Me-His-OH, where only 2 equiv of amino acid and HBTU were used). Fmoc-deprotections and resin neutralization was achieved by 2 × 2 min. treatments with excess 1:1 piperidine:DMF. Coupling yields were monitored by quantitative ninhydrin assay,[27] and double couplings were employed for yields below 99.8%. N-terminal acetylation was achieved by treating the fully assembled and protected peptide-resins (after removal of the N-terminal Fmoc group) with a solution containing 870 μL of acetic anhydride and 470 μL of DIPEA in 15 mL of DMF (2 × 5 min treatments with enough solution to cover the resin beds). The peptide was cleaved from resin, and protecting groups were simultaneously removed by treatment for 2 h at room temperature with a solution containing 95% trifluoroacetic acid (TFA):2.5% H_2O:2.5% triisopropylsilane (TIPS) (25 mL of solution per 1 g of peptide-resin). The TFA solutions were filtered and concentrated in vacuo, and peptide was precipitated with ice cold diethyl ether, diluted with 50% A:50% B, lyophilized, and subsequently purified by semipreparative rp-HPLC using a linear gradient (0%−15% B) over 30 min.

For Ac-MARAM-NH_2, Yield = 25%. Anal. rp-HPLC (linear gradient from 0% to 100% B over 30 min.): t_R = 11.7 min. MS: obs (M + H) 620.6, calcd 620.3; obs (M + 2H)/2 310.8, calcd 310.7. For Ac-HARAH-NH_2, Yield = 30%. Anal. rp-HPLC (linear gradient from 0% to 100% B over 30 min): t_R = 6.9 min. MS: obs (M + 2H)/2 316.9, calcd 316.6.

Circular Dichroism Spectroscopy. CD measurements were made using a JASCO J-710 model spectropolarimeter routinely calibrated with (1*S*)-(+)-10-camphorsulfonic acid. Solutions of **4**−**9** were diluted to 50−200 μM in acetate buffer (10 mM, pH 4.0) for measurements. Spectra were recorded in a 0.1 cm JASCO quartz cell at room temperature (298 K) or temperature control was achieved using a Neslab RTE-111 circulating water bath. Spectra were acquired between 260 and 185 at 20 nm/min with a bandwidth of 1.0 nm; response time of 0.25, 0.50, or 1 s; resolution step width of 0.1 nm; and sensitivity of 100 mdeg. Each spectrum represents the average of four or five scans with "binomial smoothing" to reduce noise.

Peptide Concentrations. The concentrations of peptides for CD measurements were determined by the PULCON method.[28] Known amounts of peptides were dissolved in 600 μL of 9:1 H_2O:D_2O solution for PULCON experiments on a DRX-600 MHz spectrometer. First, the 90° pulse of each NMR sample was carefully measured by observing the null water signal in a standard 1D proton experiment while alternating their 360° pulse. The PULCON experiments were carried out with the remeasured 90° pulse for each peptide, with a relaxation delay of 30 s, receiver gain of 64−512, 32 scans, and 298 K. The water signal was suppressed using the Watergate pulse sequence. The NMR spectrum was processed in TopSpin v1.3 with manual phase correction, and selected peptide signals were integrated for concentration calculations. Signals for the imidazole side chain of a 4.18 mM histidine solution were the reference in the calculation.

CD Calculations. The equation[29] often used to quantify the percentage of α-helical content in a peptide or protein is

$$f_H = ([\theta]_{obs222} - [\theta]_C)/([\theta]_{\infty 222} - [\theta]_C)$$

where the temperature dependent random coil molar ellipticity ($[\theta]_C$) is

$$[\theta]_C = 2220 - 53T$$

and the infinite α-helix molar ellipticity ($[\theta]_\infty$) is

$$[\theta]_{\infty 222} = (-44000 + 250T)(1 - k/N_p)$$

where T is temperature (°C), N_p is number of amino acid residues in the peptide, and k is a finite length correction. Here, the minima occurs at 218 nm, so $[\theta]_{218}$ has been used in place of $[\theta]_{222}$.

The difficulty in quantifying α-helicity using this equation involves determining an accurate value of k, which has been assigned values from 2.4 to 4.5.[30] It has been suggested that k = 3.0 for carboxyamidated peptides and that k = 4.0 for unblocked peptides.[31] Applying these two values of k and $[\theta]_{218} = -10\,804$ at 25 °C to calculating f_H for **9** gives values of f_H from 73% to 139% helicity. Given that **9** shows no increase in helicity upon increasing TFE from 20% to 50% and that NMR evidence suggests that **9** is strongly helical, it is entirely plausible that **9** is 100% helical in a solution comprised of 20% TFE/80% acetate buffer. In that case, a value of ∼3.2 can be derived for k. By applying this to **9** in 100% acetate buffer at 25 °C (where $[\theta]_{218} = -10\,781$ deg mol^{-1} cm^2 $residue^{-1}$), f_H = 82% is obtained.

One of the inherent problems with this derivation is that it is based on a study where the calculation of helicity is calibrated for 222 nm (while the equivalent minimum of **9** occurs at 218 nm). Furthermore, the study does not reflect the properties of short peptides. If instead, we assume that the metallopeptide **9** reaches its maximum helicity in a solution comprising 20% TFE/80% acetate buffer and then helicity can be determined for **6**−**11** in 100% acetate buffer at 25 °C relative to **3** at maximum helicity. For **9** in 20% TFE, $[\theta]_{218} = -13\,200$ deg mol^{-1} cm^2 $residue^{-1}$. For **9**, **8**, **7**, and **6** in a 100% aqueous solution, $[\theta]_{218} = -10\,781$, −2293, −10 080, and −1874 deg mol^{-1} cm^2 $residue^{-1}$. Therefore, for **9**, **8**, **7**, and **6** in a 100% aqueous solution, f_H = 82%, 17%, 76%, and 14%.

NMR Spectroscopy. The metallopeptide and peptide solutions were run in 10% D_2O/90% H_2O and the pH was adjusted to ∼4.0, using acetic acid (0.1 M) where required. The final concentration of metal complexes was 4−5 μmol of peptides in 0.5 mL of H_2O/D_2O (9:1) at pH 4.0 with 1 equiv of Ru or Pd.

1D and 2D ^{1}H NMR spectra were recorded on either a Bruker Avance DRX-500, -600, or -750 MHz spectrometer. 2D ^{1}H-spectra were recorded in phase-sensitive mode using time-proportional

(26) Pell, S. D.; Sherban, M. M.; Tramontano, V.; Clarke, M. J. *Inorg. Synth.* **1989**, *26*, 65–68.
(27) Sarin, V.; Kent, S. B. H.; Tan, J. P.; Merrifield, R. B. *Anal. Biochem.* **1981**, *117*, 147.
(28) Wider, G.; Dreier, L. *J. Am. Soc. Chem.* **2006**, *128*, 2571–2576.
(29) Luo, P. Z.; Baldwin, R. L. *Biochemistry* **1997**, *36*, 8413–8421.
(30) Wallimann, P.; Kennedy, R. J.; Kemp, D. S. *Angew. Chem., Int. Ed.* **1999**, *38*, 1290–1292.
(31) Rohl, C. A.; Baldwin, R. L. *Methods Enzymol.* **1998**, *295*, 1–26.

phase incrementation for quadrature detection in the t_1 dimension.[32] The 2D experiments included TOCSY (standard Bruker mlevtp or mlevph pulse programs) and ROESY (standard Bruker roesytp or roesyph pulse programs). TOCSY spectra were acquired over 4607 Hz with 4096 complex data points in F_2, 512 increments in F_1, and 16 scans per increment. ROESY spectra were acquired over 4607 Hz with 4096 complex data points in F_2, 512−1024 increments in F_1, and 32−64 scans per increment. TOCSY and ROESY spectra were acquired with an isotropic mixing time of 80−100 and 100−350 ms, respectively. Dqf-COSY spectra were acquired over 4607 Hz with 4096 complex data points in F_2, 256−512 increments in F_1, and 32 scans per increment. For all 2D experiments in 90% H_2O/10% D_2O, water suppression was achieved using a modified WATERGATE sequence.[33] For 1D ^{1}H NMR spectra in water, the water resonance was suppressed by low-power irradiation during the relaxation delay (1.5 s). Spectra were processed using TOPSPIN (Bruker, Germany) software. The t_1 dimensions of all TOCSY and ROESY spectra were zero-filled to 1024 real data points with 90° phase-shifted QSINE bell window functions applied in both dimensions followed by Fourier transformation and fifth-order polynomial baseline correction. ^{1}H chemical shifts were referenced to DSS (δ 0.00 ppm) in water. $^3J_{NHCH\alpha}$ coupling constants were measured from high-resolution 1D ^{1}H and also from 2D *dqf*-COSY spectra, where they are necessary.

The 50.68 MHz ^{15}N NMR spectra (Supporting Information) were obtained at 298 K using a DEPT pulse sequence on a Bruker Advance DRX-500 spectrometer fitted with a 5 mm broad band tunable probe. ^{15}N chemical shifts were referenced externally to the $^{15}NH_4^+$ signal (0.0 ppm) from 5 M $(^{15}NH_4)_2SO_4$ in 1 M H_2SO_4, in a coaxial capillary.

NMR Structure Calculation by Simulated Annealing/ Energy Minimization. Structural Restraints. Distance restraints used in calculating a solution structure for **9** in water were derived from ROESY spectra (recorded at 298 K) using mixing times of 200−350 ms. ROE cross-peak volumes were classified manually as strong (upper distance constraint ≤2.7 Å), medium (≤3.5 Å), weak (≤5.0 Å), and very weak (≤6.0 Å), and standard pseudoatom distance corrections[34] were applied for nonstereospecifically assigned protons. To address the possibility of conformational averaging, intensities were classified conservatively and only upper distance limits were included in the calculations to allow the largest possible number of conformers to fit the experimental data. Backbone dihedral angle restraints were inferred from $^3J_{NHCH\alpha}$ coupling constants. For $^3J_{NHCH\alpha} \leq 6$ Hz, ϕ was restrained to $-65 \pm 25°$. No restraints were included for residues with $6 \leq {}^3J_{NHCH\alpha} \leq 8.5$ Hz, because of the problem of multiple solutions to the Karplus equation over this range.[35] No evidence for *cis*-peptide amides (i.e., no CHα-CHα i, $i+1$ ROEs) was present in the ROESY spectra for the complexes, so all ω-angles were set to trans ($\omega = 180°$). Structures were initially calculated without any explicit hydrogen-bond restraints to prevent structure biasing.

Structure Calculation. The three-dimensional structure of the peptide backbone in complex **9** was calculated [without $Ru(NH_3)_4^{2+}$] using a dynamic simulated annealing and energy minimization protocol in the program X-PLOR 3.851. The starting structure of **9** with randomized ϕ and ψ angles and side chains was generated using an ab initio simulated annealing protocol.[36] The calculations were performed using the standard force field parameter set (PARALLHDG5.3.PRO) and topology file (TOPALLHDG5.3.PRO) in X-PLOR, which included in-house modifications to produce 50 structures. Refinement of the structures was achieved using the conjugate gradient Powell algorithm with 4000 cycles of energy minimization and a refined force field based on the program CHARMm.[37] The final 20 structures chosen to represent the lowest energy conformations for **9** contained no distance violations ≥0.2 Å and no dihedral violations ≥3°. Structures were displayed in Insight II (Version 2000.1, Accelrys, San Diego, CA).

Cyclic Voltammetry. The metallopeptide solutions (2 mM) were run in aqueous solutions with $NaClO_4$ (100 mM) as the supporting electrolyte. Cyclic voltammograms were acquired using Metrohm 757 VA Computrace electrochemical equipment with a glassy carbon working electrode, a platinum wire auxiliary electrode, and a Ag/Ag^+(3 M KCl) reference electrode. Solutions were purged with N_2 prior to measurement.

Acknowledgment. We thank the Australian Research Council for partial financial support, including a federation fellowship to D.P.F.

Supporting Information Available: Detailed NMR, MS, and CD spectroscopic data (13 Figures, 2 Tables). This material is available free of charge via the Internet at http://pubs.acs.org.

JA900047W

(32) Marion, D.; Wüthrich, K. *Biochem. Biophys. Res. Commun.* **1983**, *113*, 967–974.
(33) Piotto, M.; Saudek, V.; Sklenar, V. *J. Biomol. NMR* **1992**, *2*, 661–665.
(34) Wüthrich, K.; Billeter, M.; Braun, W. *J. Mol. Biol.* **1983**, *169*, 949.
(35) Mierke, D. F.; Huber, T.; Kessler, H. *J. Comput. Aided. Mol. Des.* **1994**, *8*, 29–40.
(36) Nilges, M.; Gronenborn, A. M.; Brünger, A. T.; Clore, G. M. *Protein Eng.* **1988**, *2*, 27.
(37) Brooks, B. R.; Bruccoleri, R. E.; Olafson, B. D.; States, D. J.; Swaminathan, S.; Karplus, M. *J. Comput. Chem.* **1983**, *4*, 187.